Available online at www.sciencedirect.com
SCIENCE DIRECT®
Earth and Planetary Science Letters 243 (2006) 61–73
EPSL
www.elsevier.com/locate/epsl

# Evidence for molecular size dependent gas fractionation in firn air derived from noble gases, oxygen, and nitrogen measurements

C. Huber [a,1], U. Beyerle [a,2,3], M. Leuenberger [a,*], J. Schwander [a,4], R. Kipfer [b,c,5], R. Spahni [a,4], J.P. Severinghaus [d,6], K. Weiler [a,4]

[a] *Climate and Environmental Physics, University of Bern, CH-3012 Bern, Switzerland*
[b] *Department of Water Resources and Drinking Water, EAWAG, CH-8600, Dübendorf, Switzerland*
[c] *Isotope Geology, ETH Zürich, CH-8092 Zürich, Switzerland*
[d] *Scripps Institution of Oceanography, University of California, San Diego, La Jolla, California 92093-0244, USA*

Received 22 September 2004; received in revised form 8 December 2005; accepted 15 December 2005
Available online 15 February 2006
Editor: E. Bard

**Abstract**

We present elemental and isotopic measurements of noble gases (He, Ne, Ar, Kr, and Xe), oxygen and nitrogen of firn air from two sites. The first set of samples was taken in 1998 at the summit of the Devon Ice Cap in the eastern part of Devon Island. The second set was taken in 2001 at NGRIP location (North Greenland).

He and Ne are heavily enriched relative to Ar with respect to the atmosphere in the air near the close-off depth at around 50–70 m. The enrichment increases with depth and reaches the maximum value in the deepest samples just above the zone of impermeable ice where no free air could be extracted anymore. Similarly, elemental ratios of $O_2/N_2$, $O_2/Ar$ and $Ar/N_2$ are increasing with depth. In contrast but in line with expectations, isotopic ratios of $^{15}N/^{14}N$, $^{18}O/^{16}O$, and $^{36}Ar/^{40}Ar$ show no significant enrichment near the close-off depth.

The observed isotopic ratios in the firn air column can be explained within the uncertainty ranges by the well-known processes of gravitational enrichment and thermal diffusion. To explain the elemental ratios, however, an additional fractionation process during bubble inclusion has to be considered. We implemented this additional process into our firn air model. The fractionation factors were found by fitting model profiles to the data. We found a very similar close-off fractionation behavior for the different molecules at both sites. For smaller gas species (mainly He and Ne) the fractionation factors are linearly correlated to the molecule size, whereas for diameters greater than about 3.6 Å the fractionation seems to be significantly smaller or even negligible. An explanation for this size dependent fractionation process could be gas diffusion through the ice lattice.

* Corresponding author. Tel.: +41 31 631 44 70; fax: +41 31 631 87 42.
*E-mail addresses:* huber@climate.unibe.ch (C. Huber), urs.beyerle@psi.ch (U. Beyerle), leuenberger@climate.unibe.ch (M. Leuenberger), schwander@climate.unibe.ch (J. Schwander), kipfer@eawag.ch (R. Kipfer), spahni@climate.unibe.ch (R. Spahni), jseveringhaus@ucsd.edu (J.P. Severinghaus), weiler@climate.unibe.ch (K. Weiler).
[1] Tel.: +41 31 631 85 64; fax: +41 31 631 87 42.
[2] Present address: Paul Scherrer Institute PSI, CH-5232 Villingen, Switzerland.
[3] Tel.: +41 56 310 36 39; fax: +41 56 310 32 94.
[4] Tel.: +41 31 631 44 76; fax: +41 31 631 87 42.
[5] Tel.: +41 44 823 55 30/31/32; fax: +41 44 823 52 10.
[6] Tel.: +1 858 822 2483; fax: +1 858 822 3310.

0012-821X/$ - see front matter 
doi:10.1016/j.epsl.2005.12.036

At Devon Island the enrichment at the bottom of the firn air column is about four times higher compared to NGRIP. We explain this by lower firn diffusivity at Devon Island, most probably due to melt layers, resulting in significantly reduced back diffusion of the excess gas near the close-off depth.

The results of this study considerably increase the understanding of the processes occurring during air bubble inclusion near the close-off depth in firn and can help to improve the interpretation of direct firn air measurements, as well as air bubble measurements in ice cores, which are used in numerous studies as paleo proxies.


*Keywords:* firn; firn air; firn-ice transition; fractionation; diffusion; noble gases

## 1. Introduction

The top of ice sheets consists of a porous and therefore permeable firn layer. This firn layer, where atmospheric air is moving primarily by molecular diffusion, is normally 50–100 m deep [1]. At the bottom of the firn column the firn is continuously transformed into ice thereby trapping the atmospheric air in bubbles. Measurements of the entrapped air from ice cores has been used successfully in numerous studies as a climate archive, e.g., to reconstruct greenhouse gas concentration histories [2–7], to asses the amplitude of rapid temperature changes by measuring isotopic fractionation of $N_2$ and Ar isotope ratios caused by the process of thermal diffusion in the firn column [8–12], or to date ice cores using measurements of $O_2$ isotope ratios as well as elemental ratios of $O_2/N_2$ [13,14]. Other studies have reconstructed atmospheric concentration histories of various gases from air sampled directly from the firn [15–20]. Other recent studies have been concentrated on the processes that can alter the composition of atmospheric air moving from the surface to the close-off depth where the air is finally trapped in bubbles. This study focuses on the mechanisms occurring during bubble inclusion within the firn–ice transition zone. Up to now three processes are known which modify the composition of atmospheric air in the firn column. These processes are (i) the concentration diffusion [21,22], (ii) the gravitational enrichment [1,23], and (iii) the thermal diffusion [24,25].

Firn air samples were taken from two different sites, i.e., Devon Island (Canada) and North GRIP (Greenland). The samples of the latter site give an ideal link between today's condition and former situations. A broad variety of concentrations and isotopic ratios of inert atmospheric gases were analyzed and compared with model predictions. Isotopic ratios agreed generally well with theory. However, some elemental ratios significantly differ from the model predictions and could only be explained by assuming an additional size dependent fractionation during bubble inclusion, as discussed by Bender et al. [26], Battle et al., [17] Severinghaus and Brook [27], Severinghaus and Battle [28], Bender [14], Leuenberger et al. [29], and Severinghaus et al. [30].

## 2. Sampling and analysis

Firn air samples were taken by the "bladder method" originally designed and described by Schwander et al. [15]. This method was improved during several firn air studies including the so-called "Bender-baffle" to prevent blocking of the gas flow by icing of the intake. The quality of the sampling was continuously monitored with an infrared $CO_2$ analyzer. Filling of flasks (6 l Silco steel containers) was started after reaching a stable $CO_2$ level through DEKABON tubing. After taking the sample, the bladder was removed from the borehole and drilling to the next sampling depth was performed.

The first drilling site is located at the summit of the Devon Ice Cap (approximately 75°N, 82°W, altitude: 1800 m asl.), in the east part of Devon Island (North-West Territories of Canada). This small ice cap has survived the glacial retreat since the Last Glacial Maximum. Accumulation rate is of the order of 30 cm of water equivalent per year. Despite a fairly low mean annual temperature of −23 °C, summer melting is quite frequent at this site, generating ice layers of 0.5 to 6 cm thickness, with largely varying horizontal extent (a few cm to a few m). The Devon Island firn air sampling was carried out in April 1998 during the FIRETRACC project. Successful sampling was achieved to a depth of 59 m. Impermeable ice, defined as ice from which no gas could be retrieved by pumping on it, was found at about 62 m. Sampling below 59 m was not possible both because of very low flow rate and because of unstable $CO_2$ levels.

The second set of samples was taken between May and June 2001 in the center of Greenland at the NGRIP (North GReenland Icecore Project) location (75.10 °N, 42.38 °W, altitude: 2960 m asl). The average air temperature at NGRIP is −31.6 °C and the average ice accumulation rate is 17.5 cm $H_2O$ per year. Our deepest samples for our gas analysis was taken at 71.75 m.

Table 1
Characteristics of the two sampling sites (Devon Island, NGRIP) used in the firn air model

| | Unit | Devon Island | NGRIP |
|---|---|---|---|
| Location | | 75° N, 82° W | 75.1 °N, 42.3 °W |
| Altitude | [m] | 1800 | 2960 |
| Mean air temperature | [°C] | −23.0 | −31.7 |
| Mean atmospheric pressure | [hPa] | 792 | 665 |
| Accumulation rate | [cm $H_2O$/yr] | 27.6 | 17.5 |
| Firn density at surface | [g/cm$^3$] | 0.40 | 0.32 |
| Firn density at close off | [g/cm$^3$] | 0.838 | 0.811 |
| Close-off depth | [m] | 59 | 70 |
| Impermeable depth | [m] | 62 | 78 |

Samples at even deeper depths were taken for other laboratories. Impermeable ice conditions were found below about 78 m (Table 1).

Vertical profiles of $CO_2$ concentration and density of Devon Island and NGRIP firn are shown in Fig. 1. Density has been determined by cutting the firn core into 0.55 m pieces (bags) and measuring weight and dimensions of these bag samples.

Flasks filled with firn air were analyzed mass spectrometrically at the Climate and Environmental Physics Division of the Physics Institute, University of Bern (Switzerland) and at the Isotope Geology unit of the ETH Zürich (Switzerland) in collaboration with the Swiss Federal Institute of Environmental Science and Technology (EAWAG). Ratios of nitrogen ($^{15}N/^{14}N$), oxygen ($^{18}O/^{16}O$) and argon isotopes ($^{36}Ar/^{40}Ar$) and elemental ratios of $O_2/N_2$, $Ar/O_2$ and $Ar/N_2$ were measured by isotope ratio mass spectrometry IRMS in Bern. We used a ThermoFinnigan Delta Plus XL IRMS for the NGRIP samples. Devon Island samples were measured on a MAT-250. Samples and standards were measured using a dual inlet system. To the Devon Island measurements offsets had to be applied since the surface sample was significantly different from the atmospheric values. The reason for this offset is most probably a mass spectrometric calibration offset, however an offset due to the sampling cannot fully be ruled out. Samples could potentially be influenced by the fact that the DEKABON tubing was tested with pure helium prior to sampling as it is the case for helium (see below). Absolute concentration of noble gas isotopes ($^4He$, $^3He$, $^{20}Ne$, $^{40}Ar$, $^{86}Kr$, $^{136}Xe$) and corresponding elemental ratios were measured on a statically operated mass spectrometer at the ETH Zürich. The analytical technique is following the procedure developed for the measurement of noble gases in water samples [31]. Due

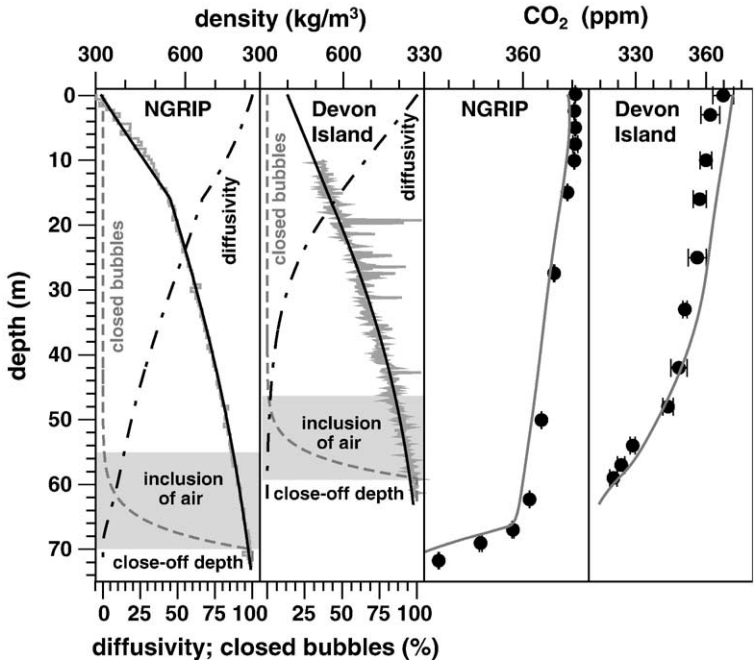


Fig. 1. (First and second panel from the left) Firn density profile of NGRIP (left) and Devon Island (right), measured (noisy gray line) and modeled (black solid line), respectively. Additionally, the modeled relative diffusivity (black chain dotted line) and the portion of closed bubbles (gray dashed line) are plotted versus depth on a percentage scale. The zone where the air inclusion takes place is marked as shaded area. They are defined as 0% to 100% of closed bubbles. (Third and fourth panel from the left) $CO_2$ measurements (circles) and model fit (solid line) of NGRIP (left) and Devon Island (right).

to the used mass spectrometric methods and the different abundances of the measured gas species, the analytical errors are two orders of magnitudes smaller for $\delta^{15}N$, $\delta^{18}O$, $O_2/N_2$ $Ar/O_2$ and $Ar/N_2$ ratios (typically between 0.01‰ to 0.05‰) compared to the static measured noble gas isotopes (typically between 4‰ to 15 ‰).

One measurement of $^{86}Kr$ from 42 m depth at Devon Island was rejected because of an unusual jump in the stability of the spectrometer (in this measurement $^{86}Kr$ was more then 9% higher than all other $^{86}Kr$ measurements). Unusual high He concentration were measured in the two uppermost Devon Island samples, 21% He excess compared to atmospheric concentration at 3 m and 7% excess He at 16 m, whereas at 33 m the He non-atmospheric excess has been completely vanished ($0.1 \pm 1\%$). These two exceptional measurements can be explained by the fact that the DEKABON tubing used for sampling was leak-checked using pure He before leaving for the field. Although the tubes were flushed by several tens of liters before sampling some non-atmospheric He had obviously remained in the DEKABON tubes contaminating the first samples taken. Therefore the helium measurements from Devon Island at 3 and 16m are not considered in the following discussion.

## 3. Firn air model

The transport of gas in porous firn can be described with a one-dimensional diffusion equation [21,22,25]:

$$\frac{\partial C}{\partial t} = \frac{\partial}{\partial z}\left(D(z,T)\left[\frac{\partial C}{\partial z} - \frac{\Delta m g}{RT} + \Omega\frac{\partial T}{\partial z}\right]\right) \quad (1)$$

where $C$ is the concentration of the species, $t$ the time, $z$ the depth, $D$ the effective molecular diffusivity of gas in porous snow as determined by direct air diffusion determination [1] or by matching model profiles to measured firn air or ice data [1,15,32], $T$ the temperature, $\Delta m$ the mass difference of the gas to the mass of air, $g$ the gravitational acceleration, $R$ the ideal gas constant, and $\Omega$ the thermal diffusion sensitivity.

In Eq. (1) the movement of gas is determined by molecular diffusion (driven by the concentration gradient $\partial C/\partial z$), by gravitational settling ($\Delta m g/RT$), and by thermal diffusion ($\Omega\ \partial T/\partial z$). As first order approximation, we did not take into account seasonal atmospheric temperature variations as well as the industrial temperature increase and geothermal flow. In this simplified model the temperature in the firn column, which is equal to the mean annual atmospheric temperature, does not change with depth or time ($\partial T/\partial z = 0$). Therefore thermal diffusion is not considered and Eq. (1) reduces to

$$\frac{\partial C}{\partial t} = \frac{\partial}{\partial z}\left(D(z,t)\left[\frac{\partial C}{\partial z} - \frac{\Delta m g}{RT}\right]\right). \quad (2)$$

Hence, Eq. (2) will fail to reproduce the gas concentrations at the upper part of the firn because seasonal atmospheric temperature variations are penetrating down to about 5–10 m depth affecting the gas concentration at the top of the firn due to thermal diffusion. However, thermal diffusion is only relevant down to a depth of about 20–30 m [25]. Since we are mainly interested in the gas concentration near the close-off depth the simplified Eq. (2) is justified. More detail about modeling firn gas movement considering thermal diffusion can be found in Severinghaus et al. [25].

To calculate the gas diffusion and inclusion process in the firn we used an extended version [32] of the one dimensional diffusion model of Schwander et al. [15]. In this model the firn column is divided into a fixed number of boxes (usually 2000), where each of the boxes contains the same mass of air. In this way we can handle the gas flow by concentration exchange (Eq. (2)). The length of the boxes thus increases with depth. The size of the boxes was determined with an approximation of the firn porosity using the density formula by Herron and Langway [33] and the relation of Schwander [21]. The gas concentration is mixed vertically between the boxes by pure molecular diffusion and the effect of gravity (Eq. (2)), as well as vertical advection due to accumulation of new surface snow. In the inclusion zone bubbles start to form, hence air is separated from the open firn column therefore decreasing the open porosity. The closed porosity is related to density by the empirical relation from Schwander et al. [1,21]. An additional process during bubble inclusion had to be implemented for this study, in order to explain the measured data. We followed the approach used by Spahni et al., [32]. In every time step a fraction of air is added to the closed pore space by removing it from the open pores at this depth. An infinitesimal change of the open porosity volume, $\Delta V$, during the integration step $j-1$ to $j$ has to be compensated by a similar change in the closed porosity, i.e.,

$$V_{\text{open}}(j) = V_{\text{open}}(j-1) - \Delta V \quad (3)$$

$$V_{\text{closed}}(j) = V_{\text{closed}}(j-1) + \Delta V. \quad (4)$$

Note, that the volume change $\Delta V$ already includes a small volume change driven by the compaction of the

firn according to the density ratio ($\rho\ (j)/\rho\ (j-1)$). Air tends to escape from the closing bubble due to a compression overpressure. In addition to Spahni et al., [32] we assumed a constant fractionation factor of the gas $i$ during bubble inclusion. The concentration $C^i_{\text{closed,new}}$ in the newly formed bubble depends on the concentration $C^i_{\text{open}}$ in the surrounding open pores as follows:

$$C^i_{\text{closed,new}}(j) = \alpha_i \cdot C^i_{\text{open}}(j-1) \tag{5}$$

where $\alpha^i$ is the fractionation factor for each gas species $i$.

Hence, to observe mass balance for this infinitesimal step Eq. (3) can be multiplied by the corresponding concentrations and results to:

$$V_{\text{open}}(j) \cdot C^i_{\text{open}}(j) = V_{\text{open}}(j-1) \cdot C^i_{\text{open}}(j-1) - \Delta V \cdot C^i{}_{\text{closed,new}}(j) \tag{6}$$

Therefore, the concentration of the remaining gas in the open pore volume $C^i_{\text{open}}\ (j)$ has to be

$$C^i_{\text{open}}(j) = C^i_{\text{open}}(j-1) \cdot [V_{\text{open}}(j-1) - \alpha_i \cdot \Delta V] \cdot (V_{\text{open}}(j-1) - \Delta V)^{-1} \tag{7}$$

according to Eqs. [(3), (5) and (6). Similarly $C^i_{\text{closed}}\ (j)$, which is the concentration in the closed pore space, can be calculated:

$$C^i_{\text{closed}}(j) = [C^i_{\text{closed}}(j-1) \cdot V_{\text{closed}}(j-1) + \alpha_i \cdot C^i_{\text{open}}(j-1) \cdot \Delta V] \cdot (V_{\text{closed}}(j-1) + \Delta V)^{-1}. \tag{8}$$

To constrain the model, we used the $CO_2$ firn air measurements (Fig. 1). The model was forced with atmospheric $CO_2$ concentration since 1750 from ice core data and measurements from Point Barrow [34]. Modeling the $CO_2$ profile is a good tool to adjust the parameters of the relation between diffusivity and open porosity used in the model [15,32]. The diffusivity profile found for $CO_2$ was then scaled linearly to the other gases (Table 2). Thereafter the concentrations of the other gases and isotopes were modeled in order to best fit the measured data by varying only the fractionation factor $\alpha_i$. This fractionation factor, $\alpha_i$, include several potential fractionations associated with the close-off process which we do not further investigate within the scope of this study but are addressed in detail in a submitted study by Severinghaus and Battle [35].

Atmospheric noble gas, oxygen and nitrogen concentrations were assumed to be constant with time. This is a simplification mostly of $O_2/N_2$ ratios, which alters seasonally due to photosynthesis and respiration processes, which is not important here as seasonal variations are not considered. Furthermore, the few atmospheric $O_2/N_2$ reconstructions suggests that the long term decrease of atmospheric $O_2/N_2$ due to fossil fuel burning, is only between 0.01‰/yr to 0.02‰/yr [36,37]. As the fractionation effect discussed in this study shows variations of 2‰ to 10‰, this latter effect is of minor importance here.

## 4. Results

### 4.1. Isotopic ratios

Both NGRIP and Devon Island firn air samples show the expected linear increase in $\delta^{15}N$, and $\delta^{18}O$ with depth due to gravitational settling. Since the gravitational enrichment is proportional to the mass difference, $\Delta m$ of the isotopes, $\delta^{36}Ar$ is affected 4 times as much as $\delta^{15}N$ (Eq. (1)). Deviations from the gravitational

Table 2
Molecular properties used in the model and close-off fractionations factors

| Molecule | Mole mass | Collision diameter[a] (Å) | $D/D(CO_2)$[b] | Close-off fractionation factor $\alpha_i$ | | | | |
|---|---|---|---|---|---|---|---|---|
| | | | | NGRIP | | Devon Island | | |
| | | | | Mean | Error | Mean | Error | Mean |
| $CO_2$ | 44 | 3.941 | 1 | 1 | | 1 | | 1 |
| Xe | 131 | 4.047 | 0.775 | 1 | | 1 | | 1 |
| $N_2$ | 28 | 3.798 | 1.21 | 1 | | 1 | | 1 |
| Kr | 84 | 3.655 | 0.944 | 1 | | 1 | | 1 |
| Ar | 40 | 3.542 | 1.22 | 0.9975 | 0.0005 | 0.9945 | 0.0015 | 0.996 |
| $O_2$ | 32 | 3.467 | 1.29 | 0.9860 | 0.0020 | 0.9855 | 0.0015 | 0.986 |
| Ne | 20 | 2.820 | 2.03 | 0.550 | 0.050 | 0.640 | 0.040 | 0.595 |
| He | 4 | 2.551 | 4.53 | 0.350 | 0.050 | 0.425 | 0.075 | 0.388 |

[a] Diameter derived from viscosity data [47].
[b] Diffusion coefficient of trace gas in air relative to $CO_2$ [42,1].

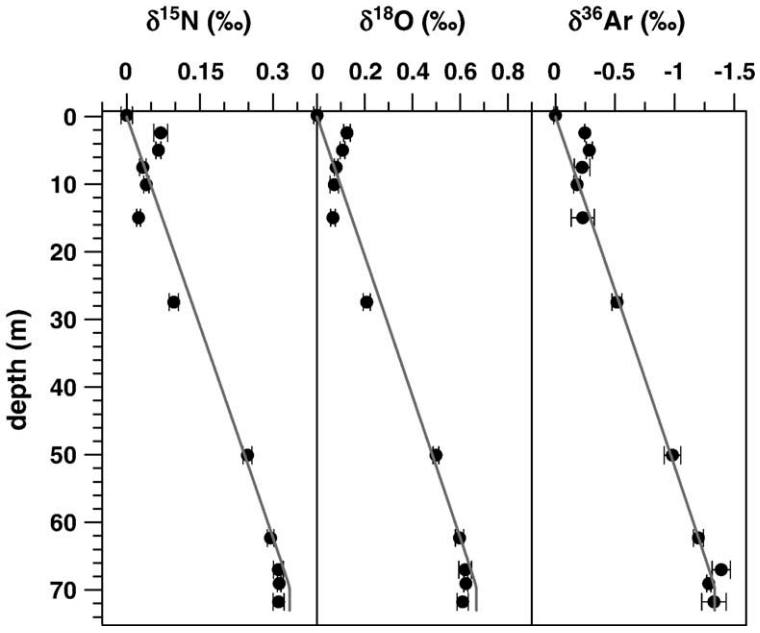


Fig. 2. Measurements (circles) and model results (solid line) for $\delta^{15}N$, $\delta^{18}O$, and $\delta^{36}Ar$ from NGRIP. The data shows a pronounced thermal effect in the upper 30 m. The model does only account for gravitational settling but not for thermal diffusion. Therefore the data and model disagree on the first 30 m.

enrichment line were observed at both sampling sites at the top of the firn air column (Figs. 2 and 3) due to thermal diffusion driven by the seasonal temperature gradients. In the present study, however, we are mainly interested at the bottom of the firn air column. For NGRIP we have no indication for close-off fractionation for isotopic ratios since they reach constant values as expected when diffusion ceases. This is confirmed by many different firn air studies at various sites in Greenland as well as in Antarctica [15,22]. However the large scatter on Devon Island samples—partly explained by lower measuring precision—does not exclude such a fractionation.

### 4.2. Elemental ratios

Measurements and model results of the elemental ratios from NGRIP and Devon Island are shown in Figs. 4–7. Model output and measurement values differ in the top 30 m because thermal diffusion is not included in the model. Below 30 m the linear gravitational shift as well as the close-off fractionation can be seen in the data and are reproduced by the model. $O_2/N_2$, $Ar/N_2$, He/Ar, Ne/Ar, Ne/He ratios show fractionations of different strengths during the inclusion process, whereas Kr/Ar and Xe/Ar seem not to be affected. Analytical errors of Kr/Ar and Xe/Ar, however, are too large to obtain a

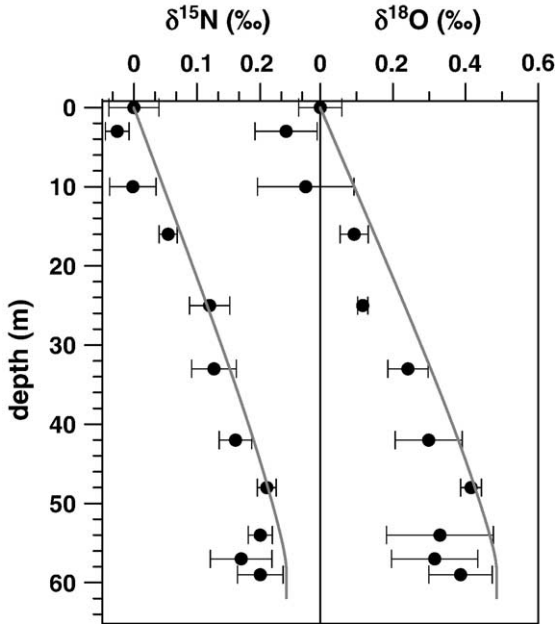


Fig. 3. Measurements (circles) and model (solid line) for $\delta^{15}N$ and $\delta^{18}O$ from Devon Island. The model does only account for gravitational settling but not for thermal diffusion. Therefore the data and model disagree on the first 30 m. The quality of the data is not as good as for NGRIP (Fig. 2).

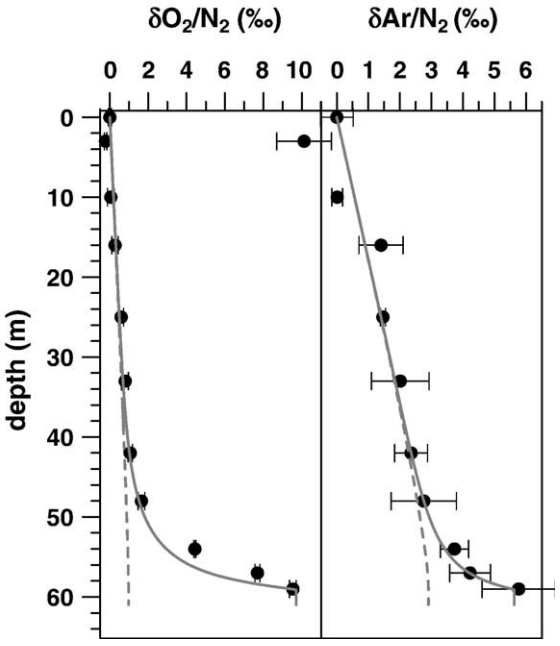


Fig. 4. $\delta O_2/N_2$ and $\delta Ar/N_2$ measurements from Devon Island. The solid lines are the diffusion model results with adjusted close-off fractionation factors whereas the dashed lines represents model results without the closed-off fractionation. Note the unusually large error for $\delta Ar/N_2$.

nice fit. The close-off enrichments are about 4 times more pronounced at Devon Island than at NGRIP. The ratio of Ne/He shows an interesting behavior, since at the close-off it is slightly enriched at NGRIP but strongly depleted at Devon Island.

Although the data from NGRIP and Devon Island are rather different, we found very similar close-off fractionation factors for both sites from fitting our model output to the data (Fig. 8). This might indicate a universal physical process of bubble inclusion. However, we do not expect these fractionation factors to be fundamental physical constants, but rather they should be affected by the speed of the bubble close-off process and are a complicated integral of the gas fractionation with the bubble pressure and close-off history. The model is able to reproduce the 4 times stronger enrichments of the He/Ar and Ne/Ar at Devon Island compared to NGRIP, as well as the different Ne/He evolutions at both sites. The reason for these differences can be found in the lower firn diffusivity at Devon Island due to intense layering obtained by frequent melt water events. This is nicely documented in the density profile (Fig. 1), which is much smoother for NGRIP than for Devon Island. Impermeable dense summer layers damp the diffusion in the firn column and hence reduce the exchange of the gases with the free atmosphere. This causes a stronger enrichment of the expelled gases from the closing bubbles in the firn, since the excess gas cannot escape easily to the atmosphere by back diffusion. Therefore, intense layering can cause a decoupling of air from the upper part of the firn column and thus lead to even stronger enrichments. Reduced

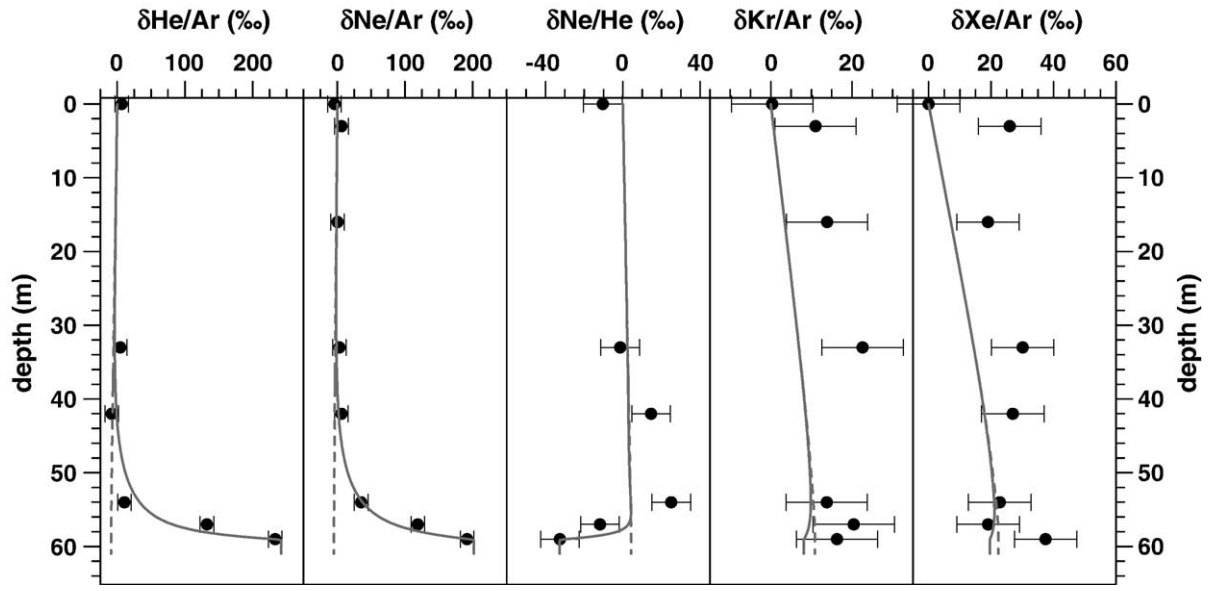


Fig. 5. Noble gas ratio measurements from Devon Island. The solid lines are the diffusion model results with adjusted close-off fractionation factors whereas the dashed lines represents model results without the closed-off fractionation.

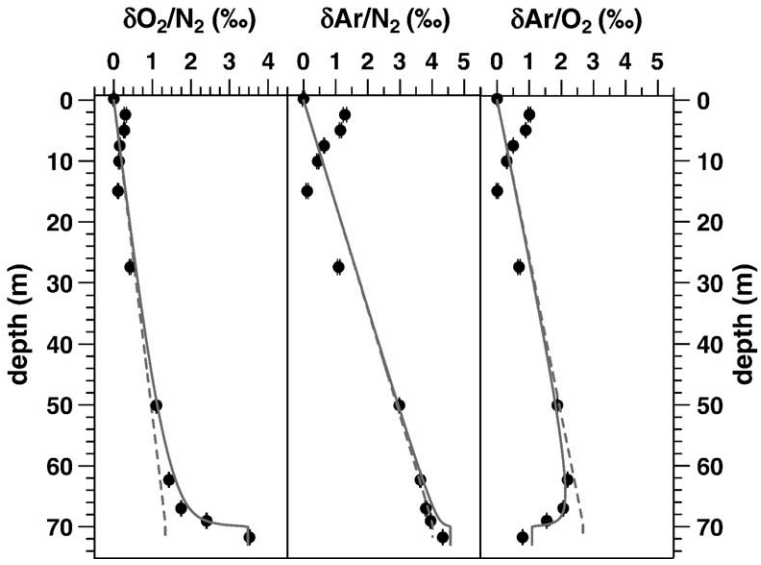


Fig. 6. $\delta O_2/N_2$, $\delta Ar/N_2$ and $\delta Ar/O_2$ measurements from NGRIP. The solid lines are the diffusion model results with adjusted close-off fractionation factors whereas the dashed lines represents model results without the closed-off fractionation.

diffusion also explains the strange behavior of the Ne/He ratios. He is more affected by the close-off fractionation than Ne, which leads to a depletion of the Ne/He ratio at Devon Island in the open pore space. In contrast, at NGRIP the Ne/He ratio is enriched at the bottom of the firn. This is because molecular diffusion of He in air is more than two times faster than of Ne in air (Table 2), hence the He concentration gradient is balanced by back diffusion to the surface at NGRIP, whereas at Devon Island reduced diffusivity due to melt layers keeps the He at the bottom of the firn. Back diffusion occurs for all enriched species, however, the effect does not lead to a change of sign as in the case of He, simply due to the fact that the close-off enrichment is significantly larger than the potential to diffuse away (see Table 2).

Close-off fractionation is strongest for the small and light elements He and Ne, and it is non-existent for the

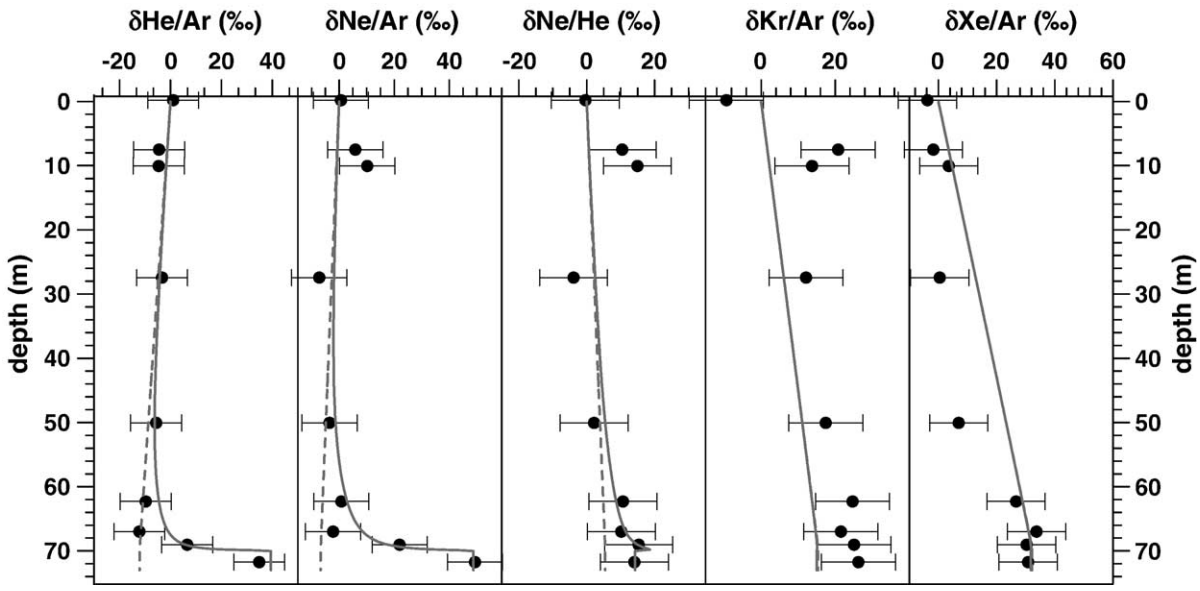


Fig. 7. Noble gas ratio measurements from NGRIP. The solid lines are the diffusion model results with adjusted close-off fractionation factors whereas the dashed lines represents model results without the closed-off fractionation.

large and heavy gases Xe and Kr, at least within our measurement precision. Plotting the close-off fractionation factor for the different species against their diameter (Fig. 8, Table 2) indicates a critical size of about 3.6 Å above which close-off fractionation seems to stop. The dependency of the close-off fractionation factor on molecular mass is not a steady function since $O_2$ (mass 32 g/mol) and Ar (40 g/mol) show stronger fractionation than the lighter $N_2$ (28 g/mol). The close-off fractionations factors obtained from the both sites agree within the uncertainty range.

In order to test the uniformity of our findings, we compared our model output for $O_2/N_2$ and $Ar/O_2$ to firn air samples from three Antarctic sites DomeC, Dronning Maud Land (DML), and Berkner Island (Fig. 9) (firn sampling within the framework of CRYOSTAT and FIRETRACC/100). Several model parameters, such as close off and surface density as well as two parameters characterizing the diffusion coefficient were calibrated again fitting the $CO_2$ profile. Then the model was run using the mean close-off fractionation factors derived from Devon Island and NGRIP (Table 2). The agreement between model and data is good for the very low accumulation (only 2.5 cm $H_2O$/yr) site of DomeC. However, Berkner Island and to a lesser extent DML data, show extremely strong close-off fractionations which could not be reproduced by the model. This is probably due to extensive non-diffusive zones as a result of impermeable layers in the firn column or to an insufficiently precise determination of model parameters via matching the measured $CO_2$ profile. Note that there are indications that part of the lower most samples from Berkner Island seem to be contaminated. The non-diffusive zone seems to start at about 50 m at Berkner Island and about 71 m at DML. This is supported by isotope ratio measurements of the four deepest samples from Berkner Island and the deepest sample at DML, respectively. The gravitational enrichment of $\delta^{15}N$ and $\delta^{18}O$ stops at this depths, whereas the samples were taken down to a depth of 63 m (Berkner Island), and 74 m (DML), respectively. Our model fails to reproduce this data, due to the smoothed diffusion profile prescribed by a smooth density profile. To improve the model, the density profile must be changed from a smooth function with depth, towards a more realistic, highly (annually) variable dependence. Such a model modification could help to improve the accuracy of reconstructions of atmospheric $O_2/N_2$ from firn air.

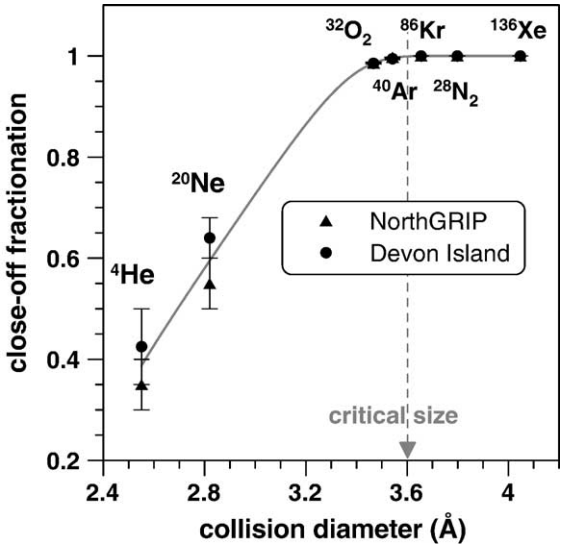


Fig. 8. Close-off fractionation factors (alpha) from the model fits of NGRIP (triangles) and Devon Island (circles), plotted against their diameter [Reid]. Close-off fractionation factors are significantly below one for small molecules, and are approaching one with increasing size. Close-off fractionation for molecules larger than the critical size of about 3.6±0.1 Å were not distinguishable from unity within the uncertainty range.

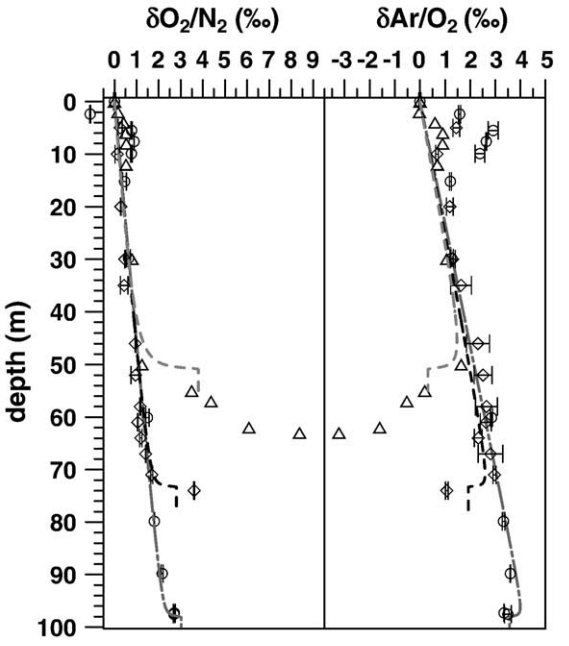


Fig. 9. $\delta O_2/N_2$ and $\delta Ar/O_2$ measurements and model predictions from the Antarctic sites DomeC (circles), DML (diamonds), and Berkner Island (triangles). For the model predictions the mean close-off fractionation factors from Table 2 were used. The Berkner Island data shows extremely strong close-off fractionation. This is probably due a very long non-diffusive zone due to impermeable layers or insufficient calibrated model parameters. This is supported by constant values of the isotope ratios for the deepest four measurements. Our model fails to reproduce this data, since layering is not yet implemented.

## 5. Discussion

The phenomenon of close-off fractionation has been discussed by several authors [14,17,26–30]. Earlier workers also noticed a size-dependent fractionation during artifactual gas loss that may occur during ice sample retrieval or storage [23,38,39]. It is important to note that this artifactual (human-caused) process is distinct from the natural process described in this work, and will not be discussed further.

During the close-off process of an air bubble the pressure in the closing bubble increases and part of the air is forced out of the bubble into the surrounding pore space. It is not clear what could cause the observed size dependence of this expelling procedure. Some kind of diffusion, such as diffusion through tiny channels in the firn structure or even through the ice matrix is probably involved. Different diffusion processes have been discussed in prior literature (Poiseuille diffusion, molecular diffusion, effusion, Knudsen diffusion, steric diffusion) [23,39], but none of them can explain the detected size dependent behavior properly.

*Poiseuille diffusion* (viscous flow) refers to a gas flow along a gradient in total pressure. There is no fractionation associated with Poiseuille diffusion, thus it does not cause the fractionation at close-off.

*Molecular diffusion* occurs in the presence of partial pressure gradients. It is important when the diameter of the channel is much bigger than the size of the molecules, thus the molecules collide much more frequently with each other than with the walls of the medium. Fractionation due to molecular diffusion depends mainly on the inverse square root of the reduced mass, $\mu$, divided by the squared diameter, $d$: $D_{\mathrm{mol}} \propto \mu^{-1/2}\ d^{-2}$. It cannot explain the observed fractionation (Fig. 8, Table 2) since otherwise isotope ratios should show a significant (detectable) fractionation. Furthermore a critical diameter cannot be explained by molecular diffusion. Molecular diffusion, however, is the driver of the back diffusion of excess gases expelled in the firn column and hence it is very important for the interpretation of the measured profiles.

*Effusion, Knudsen diffusion* occurs when the molecules collide predominantly with the walls rather than with each other, e.g., a collapsing balloon expelling the gas. Knudsen diffusion is inversely proportional to the square root of its mass: $D_{\mathrm{Knudsen}} \propto m^{-1/2}$. Therefore, this type of diffusion depends only on the square root of the mass ratio off different gases but not on the molecular size: $D_2/D_1 \propto (m_1/m_2)^{1/2}$. Neither effusion nor Knudsen diffusion can explain the size dependency, as well as the unaffected isotope ratios, observed during the inclusion process.

*Steric (activated) diffusion* is important when the size of the molecules is of the same order as the size of the channel. Then the diffusivity depends on both the diameter and the mass of the molecule: $D_{\mathrm{activated}} \propto m^{-1/2} \exp(-E/kT)$ where $E = E_0 + ad$ is the activation energy required to jump from one crystal-site to the next (see for example Kärger and Ruthven [40]). Diffusion through the ice matrix can be regarded as steric diffusion [41,42]. Hence steric or activated diffusion could be a driver of the observed close-off fractionation, however there is still a mass dependence involved.

The clear detection of a critical size of 3.6 Å implies diffusion through channels of about the same dimension. However, an outlet from a closing bubble is not expected to develop a critical size, since it changes its dimension steadily from open to closed. Furthermore, a uniform behavior of the firn structure close-off region (the same channel dimensions at different sites) seems unrealistic, since physical conditions (temperature, accumulation) can be very different from site to site. Thus, we favor an explanation by diffusion through the ice matrix. Diffusion coefficients of gases in ice show a size dependence similar to our findings beside for Ar and $O_2$ [41]. However, diffusion through ice is very slow (far less than 1 mm/yr) [41–43]. Therefore, a wall of a few tenths of millimeter can inhibit gas penetration substantially. But, one can imagine that a newly formed bubble is sealed from the open pores by only a very thin film of ice crystals. The overpressure in the bubble forces the gases to migrate through the ice structure. Diffusion through ice must behave in a uniform way, because the crystalline structure depends not much on temperature and pressure. At the pressure and temperature conditions of polar firn, normal ice (Ih) with a hexagonal crystalline structure is formed (Fig. 10). The crystal may be thought of as consecutive sheets lying on top of each other. For a very thin wall of ice (<1 μm) such a crystal structure is forming hexagonal channels, which could serve as connections for the air from the bubble to the open pore volume. The distance between two neighboring oxygen atoms is about 2.75 Å [44]. The dimensions of the hexagonal passages in the ice matrix each formed by six $H_2O$ molecules is similar to the critical size of about 3.6 Å (4.5–4.6 Å minus the dimension of the $H_2O$ molecules of about 1–2 Å) (Fig. 10). Therefore, a size dependent fractionation seems probable. Molecules larger than the channels are not able to pass the ice film, whereas small molecules like He pass easily. Bubble air measurements on ice cores by Severinghaus and Battle [28] showed that a significant

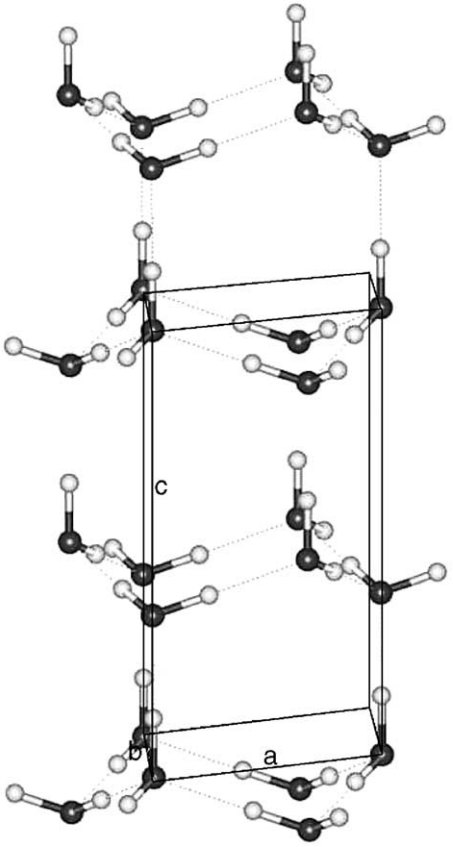


Fig. 10. Hexagonal ice (Ih) unit cell. The unit cell may be considered as a group of four molecules (two above and two below); two and two halves of which make up the hexametric box. The crystallographic *c*-axis is in the vertical direction. The hexagonal crystal has unit cell dimensions 4.511 Å (a, b) and 7.351 Å (c) (90°, 90°, 120°, 4 molecules). The distance between two neighboring oxygen atoms (dark globes) is about 2.75 Å [44].

part of He, as well as Ne are lost in ice cores, whereas $N_2$, Ar, and $O_2$ concentrations seem to remain unchanged, at least in the inner part of the core [45]. This is in agreement with older diffusion coefficient experiments [46]. But, regarding a small film of ice only, $O_2$ and Ar have a slightly higher probability to pass than $N_2$, which could cause the enrichments in the firn in the close-off region. Further investigations concerning this theory have to be carried out; in addition better experimental determinations of the diffusion constants of the main air components through ice would be very valuable.

Independent of the origin of these fractionation effects ice core data is most probably partly affected. Important are influences on elemental ratios such as $O_2/N_2$ and $Ar/N_2$. In contrast, trace gas concentrations, except light gases such as He and Ne, as well as isotopic compositions are hardly altered facing the present knowledge.

## 6. Conclusions

The enrichment of elemental ratios near the close-off region measured in the firn air from Devon Island and NGRIP, can be modeled assuming a constant close-off fractionation factor between closed off air and open pore composition during air enclosure. The strong similarities found at both sites indicate a universal physical process causing this close-off fractionation. Our model approach is able to explain and predict the general shape of the firn air profiles from various different sites. However, it fails when the firn density structure has impermeable layers that cause large non-diffusive zones at the bottom of the firn. This has to be implemented into a future model. Close-off fractionation factors for different gases depend strongly on the diameter. The mass of the molecule is less important, since the effect on isotope ratios is very low. The critical size of about 3.6 Å seems to be an upper limit up to which molecules fractionate during the close-off process in the firn. A possible explanation for this could be the diffusion of molecules through channels in the ice lattice. From our findings we believe that the effect of close-off fractionation is nonexistent or at least very small for isotope ratios and for large molecules, like Xe, Kr, $N_2$, $CO_2$, $CH_4$, and $N_2O$. This is an important confirmation for the integrity of polar ice cores as a climate archive of the ancient atmospheric composition of these gases.

## Acknowledgements

This work is a contribution to the European Commission projects FIRETRACC/100 (ENV4-CT97-0406) funded under the Environment and Climate Programme; 1994–1998, and CRYOSTAT (EVK2-CT2001-00116) funded under the Energy, Environment and Sustainable Development Programme; 1998–2002. It benefited from the field support of the French Polar Institute (IFRTP), of Roy Koerner and David Fisher of the Geological Survey of Canada (Glaciology Section), and of the Polar Continental Shelf Project (Natural Resources Canada) at Devon Island. We thank Jérôme Chappellaz for providing Devon Island detailed density measurements. The NorthGRIP project is directed and organized by the Department of Geophysics at the Niels Bohr Institute for Astronomy, Physics and Geophysics, University of Copenhagen. It is being supported by Funding Agencies in Denmark (SNF), Belgium (FNRS-CFB), France (IFRTP and INSU/CNRS), Germany (AWI), Iceland (RannIs), Japan (MEXT), Sweden (SPRS), Switzerland (SNF) and the United States of America (NSF). Furthermore we thank Peter Nyfeler for

IRMS measurements and Francesco Valentino for providing model results. The work of Eawag/ETH was supported by SNF grants 2000.067933.02/1 and 200020-107489/1.

## References

[1] J. Schwander, B. Stauffer, A. Sigg, Air mixing in firn and the age of the air at pore close-off, Ann. Glaciol. 10 (1988) 141–145.
[2] E.J. Brook, T. Sowers, J. Orchardo, Rapid variations in atmospheric methane concentration during the past 110,000 years, Science 273 (1996) 1087–1091.
[3] T. Blunier, J. Chappellaz, J. Schwander, J.-M. Barnola, T. Desperts, B. Stauffer, D. Raynaud, Atmospheric methane record from a Greenland ice core over the last 1000 years, J. Geophys. Res. 20 (20) (1993) 2219–2222.
[4] J. Chappellaz, T. Blunier, D. Raynaud, J.M. Barnola, J. Schwander, B. Stauffer, Synchronous changes in atmospheric $CH_4$ and Greenland climate between 40 and 8 kyr BP, Nature 366 (1993) 443–445.
[5] J. Flückiger, T. Blunier, B. Stauffer, J. Chappellaz, R. Spahni, K. Kawamura, J. Schwander, T.F. Stocker, D. Dahl-Jensen, $N_2O$ and $CH_4$ variations during the last glacial epoch: insight into global processes, Glob. Biogeochem. Cycles GB 1020 (2004), doi:10.1029/2003GB002122.
[6] E. Monnin, A. Indermühle, A. Dällenbach, J. Flückiger, B. Stauffer, T.F. Stocker, D. Raynaud, J.-M. Barnola, Atmospheric $CO_2$ concentrations over the last glacial termination, Science 291 (2001) 112–114.
[7] A. Indermühle, T.F. Stocker, F. Joos, H. Fischer, H.J. Smith, M. Wahlen, B. Deck, D. Mastroianni, J. Tschumi, T. Blunier, B. Stauffer, Holocene carbon-cycle dynamics based on $CO_2$ trapped in ice at Taylor Dome, Antarctica, Nature 398 (1999) 121–126.
[8] J.P. Severinghaus, E.J. Brook, Abrupt climate change at the end of the last glacial period inferred from trapped air in polar ice, Science 286 (1999) 930–934.
[9] J.P. Severinghaus, T. Sowers, E.J. Brook, R.B. Alley, M.L. Bender, Timing of abrupt climate change at the end of the Younger Dryas interval from thermally fractionated gases in polar ice, Nature 391 (1998) 141–146.
[10] M.C. Leuenberger, C. Lang, J. Schwander, Delta $^{15}N$ measurements as a calibration tool for the paleothermometer and gas–ice age differences: a case study for the 8200 B.P. event on GRIP ice. J. Geophys. Res. 104 (D18) (1999) 22163–22170.
[11] C. Lang, M. Leuenberger, J. Schwander, S. Johnsen, 16 °C rapid temperature variation in central Greenland 70,000 years ago, Science 286 (1999) 934–937.
[12] A. Landais, N. Caillon, C. Goujon, A. Grachev, J.M. Barnola, J. Chappellaz, J. Jouzel, V. Masson-Delmotte, M. Leuenberger, Quantification of rapid temperature change during DO event 12 and phasing with methane inferred from air isotopic measurements, Earth Planet. Sci. Lett. 225 (2004) 221–232.
[13] J.R. Petit, J. Jouzel, D. Raynaud, N.I. Barkov, J.-M. Barmola, I. Basile, M. Bender, J. Chapppellaz, M. Davis, G. Delaygue, M. Demotte, V.M. Kotlyakov, M. Legrand, V.Y. Lipenkov, C. Lorius, L. Pépin, C. Ritz, E. Saltzman, M. Stievenard, Climate and atmospheric history of the past 420,000 years from the Vostok ice core, Antarctica, Nature 399 (1999) 429–436.
[14] M. Bender, Orbital tuning chronology for the Vostok climate record supported by trapped gas composition, Earth Planet. Sci. Lett. 204 (2002) 275–289.
[15] J. Schwander, J.-M. Barnola, C. Andrié, M. Leuenberger, A. Ludin, D. Raynaud, B. Stauffer, The age of the air in the firn and the ice at Summit, Greenland, J. Geophys. Res. 98 (1993) 2831–2838.
[16] J.H. Butler, M. Battle, M.L. Bender, S.A. Montzka, A.D. Clarke, E.S. Saltzman, J.P. Sucher, J.P. Severinghaus, J.W. Elkins, A record of atmospheric halocarbons during the twentieth century from polar firn air, Nature 399 (1999) 749–755.
[17] M. Battle, M. Bender, T. Sowers, P.P. Tans, J.H. Butler, J.W. Elkins, J.T. Ellis, T. Cornway, N. Zhang, P. Lang, A.D. Clarke, Atmospheric gas concentrations over the past century measured in air from firn at the South Pole, Nature 383 (1996) 231–235.
[18] R.J. Francey, M.R. Manning, C.E. Allison, S.A. Coram, D. Etheridge, R.L. Langenfelds, D.C. Lowe, L.P. Steele, A history of delta C-13 in atmospheric $CH_4$ from the Cape Grim air archive and Antarctic firn air, J. Geophys. Res. 104 (1999) 23,631–23,643.
[19] D.M. Etheridge, L.P. Steele, R.J. Francey, R.L. Langenfelds, Atmospheric methane between 1000 AD and present: evidence for anthropogenic emission and climate variability, J. Geophys. Res. 103 (1998) 15,979–15,993.
[20] D.M. Etheridge, L.P. Steele, R.L. Langenfields, R.J. Francey, J.-M. Barnola, V.I. Morgan, Natural and anthropogenic changes in atmospheric $CO_2$ over the last 1000 years from air in Antarctic ice and firn, J. Geophys. Res. 101 (1996) 4115–4128.
[21] J. Schwander, The transformation of snow to ice and the occlusion of gases, in: H. Oeschger, C.C. Langway Jr. (Eds.), The Environmental Record in Glaciers and Ice Sheets, John Wiley, New York, 1989, pp. 53–67.
[22] C.M. Trudinger, I.G. Enting, D.M. Etheridge, R.J. Francey, V.A. Levchenko, L.P. Steele, D. Raynaud, L. Arnaud, Modelling air movement and bubble trapping in firn, J. Geophys. Res. 102 (D6) (1997) 6747–6763.
[23] H. Craig, Y. Horibe, T. Sowers, Gravitational separation of gases and isotopes in polar ice caps, Science 242 (1988) 1675–1678.
[24] J. Severinghaus, T. Sowers, Thermal diffusion as a temperature-change indicator in ice core climate records (abstract), EOS Trans. AGU 76 (46) (1995) F291 (Fall Meet. Suppl.).
[25] J.P. Severinghaus, A. Grachev, M. Battle, Thermal fractionation of polar firn by seasonal temperature gradients, Geochem. Geophys. Geosyst. 2 (2001) 2000GC000146.
[26] M.L. Bender, T. Sowers, J.-M. Barnola, J. Chappellaz, Changes in $O_2/N_2$ ratio of the atmosphere during recent decades reflected in the composition of air in the firn at Vostok Station, Geophys. Res. Lett. 21 (1994) 189–192.
[27] J.P. Severinghaus, E.J. Brook, Do atmospheric gases fractionate during air bubble closure in polar firn and ice? EOS Trans. AGU 81 (2000) S20.
[28] J. Severinghaus, M. Battle, Ninety per mil enrichment of neon in firn air at South Pole, Geophys. Res. Abstr. 4 (2002) EGS02-A-00510.
[29] M. Leuenberger, P. Nyfeler, J. Schwander, Isotopic and elemental ratio measurements on air from NorthGRIP firn air sampling 2001, Geophys. Res. Abstr. 4 (2002) EGS02-A-01299.
[30] J.P. Severinghaus, A. Grachev, B. Luz, N. Caillon, A method for precise measurement of argon 40/36 and krypton/argon ratios in trapped air in polar ice with applications to past firn thickness and abrupt climate change in Greenland and at Siple Dome, Antarctica, Geochim. Cosmochim. Acta 67 (3) (2003) 325–343.

[31] U. Beyerle, W. Aeschbach-Hertig, D.M. Imboden, H. Baur, T. Graf, R. Kipfer, A mass spectrometric system for the analysis of noble gases and tritium from water samples, Environ. Sci. Technol. 34 (2000) 2042–2050.
[32] R. Spahni, J. Schwander, J. Flückiger, B. Stauffer, J. Chappellaz, B. Raynaud, The attenuation of fast atmospheric $CH_4$ variations recorded in polar ice cores, Geophys. Res. Lett. 30 (11) (2003) 1571, doi:10.1029/2003GL017093.
[33] M.M. Herron, C.C. Langway Jr., Firn densification: an empirical model, J. Glaciol. 25 (1980) 373–385.
[34] GLOBALVIEW-$CO_2$, Cooperative atmospheric data integration project — carbon dioxide. CD-ROM, NOAA CMDL, Boulder, Colorado [Also available on Internet via anonymous FTP to ftp.cmdl.noaa.gov, Path: ccg/co2/GLOBALVIEW] (2004).
[35] J.P. Severinghaus, M. Battle, Fractionation of gases in polar ice during bubble close-off: new constraints from firn air Ne, Kr, and Xe observations, Earth Planet. Sci. Lett. (submitted for publication).
[36] C.D. Keeling, S.C. Piper, M. Heimann, Global and hemispheric $CO_2$ sinks deduced from changes in atmospheric $O_2$ concentration, Nature 381 (1996) 218–221.
[37] M.L. Bender, J.T. Ellis, P.P. Tans, R.J. Francey, L.D., Variability in the $O_2/N_2$ ratio of southern hemisphere air, 1991–1994: implications for the carbon cycle, Glob. Biogeochem. Cycles 10 (1) (1996) 9–21.
[38] T.A. Sowers, M.L. Bender, D. Raynaud, Elemental and isotopic composition of occluded $O_2$ and $N_2$ in polar ice, J. Geophys. Res. 94 (1989) 5137–5150.
[39] M. Bender, T. Sowers, V. Lipenkov, On the concentraion of $O_2$, $N_2$, and Ar in trapped gases from ice cores, J. Geophys. Res. 100 (D9) (1995) 18651–18660.
[40] J. Kärger, D.M. Ruthven, Diffusion in Zeolites and other Microporous Solids, John Wiley and Sons, Inc, New York, 1992.
[41] T. Ikeda, H. Kukazawa, S. Mae, L. Pepin, P. Duval, B. Champagnon, V. Lipenkov, T. Hondoh, Extreme fractionation of gases caused by formation of clathrate hydrates in Vostok Antarctic ice, Geophys. Res. Lett. 26 (1) (1999) 91–94.
[42] T. Uchida, S. Mae, T. Hondoh, V.Y. Lipenkov, P. Duval, J. Kawabata, Growth process of air-hydrates and diffusion of air molecules in deep ice sheet, Proc. NIPR Symp. Polar Meteorol. Glaciol. 8 (1994) 140–148.
[43] T. Ikeda-Fukazawa, K. Fukumizu, K. Kawamura, T. Nakazawa, T. Hondoh, Effects of molecular diffusion on trapped gas compositions in polar ice cores, Earth Planet. Sci. Lett. 229 (2005) 183–192.
[44] A. Goto, T. Hondoh, S. Mae, The electron density distribution in ice Ih determined by single-crystal X-ray diffractometry, J. Chem. Phys. 93 (2) (1990) 1412–1417.
[45] N. Caillon, J. Severinghaus, J. Chappellaz, J. Jouzel, V. Masson-Delmotte, Impact of refrigeration temperature history on $\delta^{15}N$ of air bubbles trapped in polar ice samples, Notes des Activités instrumentales IPSL 14 (2001).
[46] P.V. Hobbs, Ice Physics, Clarendon Press, Oxford, 1974, 837 pp.
[47] R.C. Reid, T.K. Sherwood, The Properties of Gases and Liquids, McGraw-Hill, New York, 1966.